Title

In situ measurement of the hydrulic diffusivity of the active Chelungpu Fault, Taiwan

Journal

Geophysical Research Letters, 33(L16317)

Authors

Doan, Mai-Linh
Brodsky, Emily E.
Ma, Kuo-Fong
et al.

Publication Date

2006-08-30

Peer reviewed

In situ measurement of the hydraulic diffusivity of the active Chelungpu Fault, Taiwan

M. L. Doan,[1,2] E. E. Brodsky,[1] Y. Kano,[3] and K. F. Ma[2]

Received 12 May 2006; revised 11 July 2006; accepted 17 July 2006; published 30 August 2006.

[1] Hydraulic diffusivity controls fluid pressure and hence affects effective normal stress during rupture. Models suggest a particularly spectacular example of fluid pressurization during the M_w = 7.6 1999 Chichi earthquake when pressurization may have reduced high-frequency shaking in the regions of large slip if the fault was sufficiently sealed. We investigate in situ hydraulic diffusivity which is the key parameter in such models through a cross-hole experiment. We find a diffusivity of $D = (7 \pm 1) \times 10^{-5}$ m^2/s, which is a low value compatible with pressurization of the Chelungpu fault during the earthquake. In most poroelastic media, the hydraulic storativity S lies between 10^{-7} and 10^{-5}, so that the transmissivity T along the fault zone is comprised between 10^{-11} m^2/s and 10^{-9} m^2/s. The corresponding permeability (10^{-18}–10^{-16} m^2) is at most one hundred times larger than the value obtained on core samples from the host rock. The fault zone is overpressurized by 0.06 to 6 MPa, which is between 0.2% and 20% of the lithostatic pressure. **Citation:** Doan, M. L., E. E. Brodsky, Y. Kano, and K. F. Ma (2006), In situ measurement of the hydraulic diffusivity of the active Chelungpu Fault, Taiwan, *Geophys. Res. Lett.*, *33*, L16317, doi:10.1029/2006GL026889.

1. Introduction

[2] The hydraulic diffusivity of the damage zone is a fundamental property of earthquake rupture because it controls the fluid overpressure that can be maintained on a fault. In between earthquakes, this fluid pressure can control failure [*Sibson et al.*, 1975; *Nur and Booker*, 1972]. For rupture during earthquakes, *Rice* [2006] and *Andrews* [2002] both calculated that the length scale over which slip weakening occurs depends critically on the hydraulic diffusivity. Cycles of healing and damage in rocks affect permeability which is dominated by fractures [*Ben-Zion and Sammis*, 2003].

[3] Permeability, which is the most variable part of hydraulic diffusivity (see description of variables in Text S1 of the auxiliary material[1]), is controlled by the fractures in the heavily brecciated fault damage zone surrounding the fault core [*Caine et al.*, 1996]. Laboratory measurements of core samples give a lower bound on the diffusivity [*Lockner et al.*, 2005; *Tanikawa et al.*, 2005; *Chen et al.*, 2005; *Kitamura et al.*, 2005], but permeability is notoriously scale dependent [*Townsend and Zoback*, 2000; *Manning and Ingebritsen*, 1999]. The most important fractures may be on scales much larger than a core sample and therefore it is necessary to measure the properties in situ.

[4] Despite the fundamental importance of hydraulic diffusivity, it has never been successfully measured in situ on an active large-scale fault. Hydraulic tests in deep boreholes intersecting the Nojima fault were attempted by *Kitagawa et al.* [1999, 2002] but they were tapping flow in the hanging wall at least 50 m away from the fault core and therefore at the diffuse end of the damaged zone. In the present study, we study a pair of boreholes intersecting the Chelungpu fault that are perforated closer to the fault core.

[5] Water was pumped out of hole A (Figure 1). The resulting head change propagated along the fault zone to produce a hydraulic anomaly in hole B. We report the results of the experiment and discuss a number of significant complications related to leaks in the well casing. After effectively modeling the leaks, we extract a value of diffusivity for the fault damage zone of $\sim 7 \times 10^{-5}$ m^2/s, which is sufficiently low to confine pressurized fluid during an earthquake.

2. Hydraulic Tests on the Chelungpu Fault

2.1. Boreholes of the Taiwan Chelungpu-Fault Drilling Project

[6] The pair of boreholes used for this experiment are separated by 40 m. Both holes are fully cased and cemented in their annuli. Both are perforated only near their intersection with the Chelungpu fault. Hole A is perforated directly above the fault; hole B directly below (Figure 1).

[7] The first borehole (hole A) intersects the fault at a depth of 1111 m within the silty shales of the Chinshui formation, that are sandwiched between the sandstone dominated rocks of the Cholan and Kueichulin formations (Figure 1). The slip is concentrated within a 12 cm thin layer of fine-grained clayish "black material", which is distinct from the nearby 30 cm thick layer of grayish gouge. The other hole (hole B) intersects regions of black material that are also interpreted as slip zones at 1137.5 m and 1138.0 m [*Ma et al.*, 2005]. In both holes, the fault core is surrounded by breccia and fractured rocks that form a 1-m wide damage zone.

2.2. Pumping Test

[8] We pumped water out of hole A on Nov. 18, 2005 and then continuously recorded the water level in both holes for the following 3 months. The pumping was as fast as

[1]Earth Science Department, University of Santa Cruz, Santa Cruz, California, USA.
[2]National Central University, Chung-li, Taiwan.
[3]Disaster Prevention Research Institute, Kyoto University, Kyoto, Japan.

0094-8276/06/2006GL026889

[1]Auxiliary materials are available in the HTML. doi:10.1029/2006GL026889.

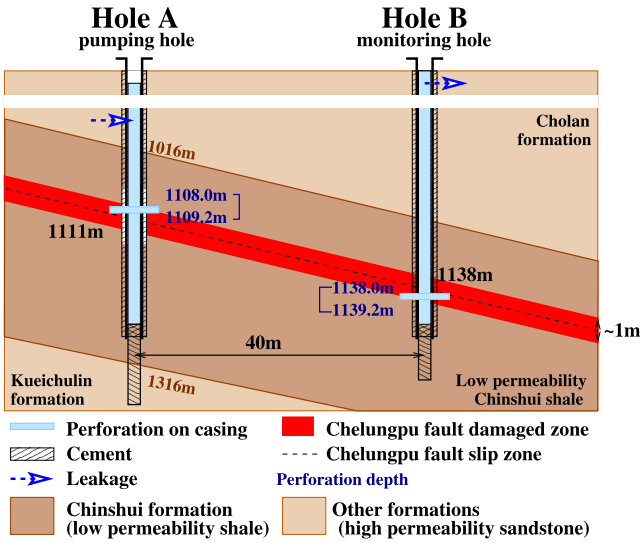

Figure 1. Configuration of the cross-hole hydraulic test on the Chelungpu boreholes. The two holes are separated by 40 m and perforated near the fault with a density of 4 shots per foot. Blue thick numbers indicate the top and bottom depths of the perforations. Perforation location is accurate to within 0.5 m. This schematic is not true scale.

permitted by the hydraulic equipment (about 60 gpm$\sim$ 4×10^{-3} m^3/s) and its duration was limited to 45 minutes. Figure 2 shows the evolution of water level in hole A during and after the pumping. The water level in the

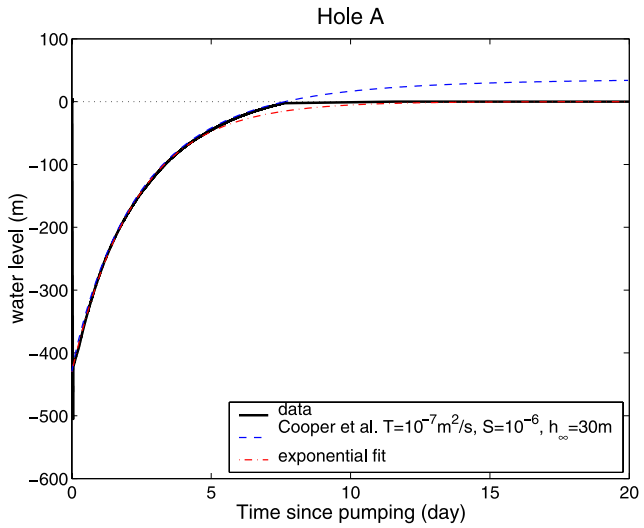

Figure 2. Recovery of the water level in the pumping hole through time. We lowered the water level of hole A by 400 m. (There was a small transient that dropped the level to −500 m while the pump was deployed). The curve fits the evolution predicted by *Cooper et al.* [1967] with the transmissivity $T = 10^{-7}$ m^2/s and the storativity $S = 10^{-6}$ (blue dashed curve), provided we take into account the overpressure of the leaky aquifer (about 0.3 MPa, equivalent to 30 m of water). This theoretical result does not take into account the fixed level of head at the surface. The red dot-dashed curve depicts the exponential function used in equation (A4) of the auxiliary material to compute analytically the expected response of hole B.

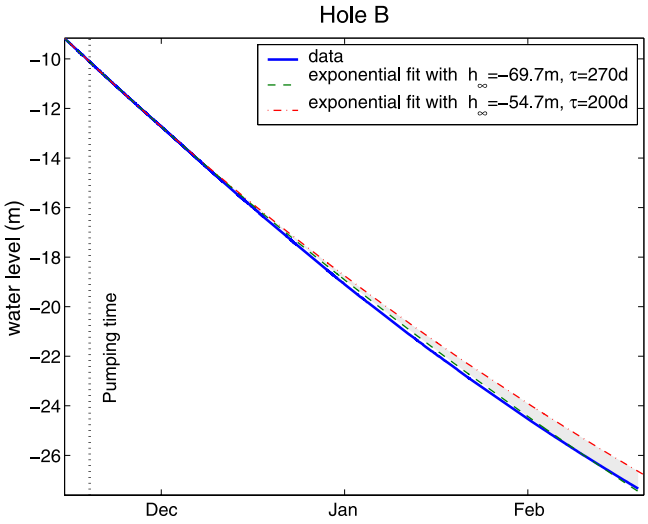

Figure 3. Evolution of the water level in hole B relative to the wellhead. It is compared with the exponential solutions computed with equation (2). We present here the two extreme sets of parameters τ = 200 days, $h_\infty = -54.7$ m (top red dot-dashed line) and τ = 270 days, $h_\infty = -69.7$ m (bottom green dashed line), that delineate a range of possible fitting exponentials (shaded area). The maximum departure is 70 cm, over a total change of 18 m. The error is thus less than 3.5% over 3 months.

pumping well recovered in one week and then stayed at zero when it reaches the wellhead.

[9] Figure 3 shows the evolution of water level in hole B. Both before and after pumping, the water level continuously decreased due to leaks in the casing resulting in a loss of more than 18 m in 3 months. This large loss from leakage obscures the more subtle drop in water level that was created by the pumping in hole A. Therefore, we need to model and remove the effects of the leaks in hole B so that we can then detect the transient induced by the pumping.

3. Analysis

[10] To recover the hydraulic properties of the fault zone, we analyze how the monitoring well (hole B) responds to the pumping well (hole A). We: (1) model the recovery of water level in hole A, which is the cause of the anomaly in hole B, (2) remove the effects of the leaks in hole B and (3) compare the remaining anomaly with a prediction based on the variations in water level in hole A to recover the hydraulic properties of the fault zone.

3.1. Modeling the Pumping Hole

[11] The sudden change in water level from the pumping in hole A disturbed the aquifers tapped by the well. For a single isotropic poroelastic aquifer with no lateral boundaries, *Cooper et al.* [1967] computed a solution (see equation (A5) of the auxiliary material). Figure 2 displays the model with the best-fit parameters, which are storativity $S = 10^{-6}$ and transmissivity $T = 10^{-7}$ m^2/s. The model of *Cooper et al.* [1967] does not take into account the overpressure in the aquifer so that the computed curve was shifted by the overpressure in the aquifer, which is 0.3 MPa (equivalent to 30 m of water).

[12] Even before the perforation, hole A was artesian with a flow rate of 10^{-6} m^3/s due to a leaky casing. Prior to perforation, a pumping test was done on hole A (C.-S. Chen, personal communication, 2005). The results suggest that the leaks tap an aquifer with an overpressurized hydraulic head of 30 to 50 m and a transmissivity close to 10^{-7} m^2/s. These values are similar to those retrieved in Figure 2, indicating that the recovery in hole A is dominated by the leakage rather than by the perforated fault zone.

[13] Although the model of *Cooper et al.* [1967] gives satisfactory results, it does not take into account the constant water level when water reaches the surface. The input signal in hole A was approximated by the exponential fit of Figure 2, which gives slower recovery than the observed data. This exponential approximation will be used in section 3.3 to fit the anomaly in hole B.

3.2. Removal of the First-Order Trend Induced by Leaks in Hole B

[14] Figure 3 shows that the water level in hole B is dominated by a continuous decrease in water level. This decrease existed prior to the perforation in hole B and is due to leakage in the casing. To extract the disturbance due to the pumping in hole A, an accurate approximation of this leakage is needed.

[15] Let us suppose a quasi-permanent radial flow inside the aquifer tapped by the leakage. The flow Q through the leak is given by the Thiem equation:

$$Q = -\frac{2\pi T}{\ln(R_\infty/r_b)}\left(h_w - h_f\right) \quad (1)$$

where R_∞ is the radius of influence beyond which the pressure in the formation is undisturbed, r_b is the borehole radius (equal to 7.8 cm for both holes A and B), T is the transmissivity of the formation, h_w is the hydraulic head in the well and h_f is the hydraulic head in the formation. Combined with the conservation of mass of fluid in the borehole, the water level in hole B is described by an exponential function:

$$h_w = h_\infty + \left(h_w(t_0) - h_\infty\right) e^{-(t-t_0)/\tau} \quad (2)$$

where $\tau = \pi r_c^2 / \frac{2\pi T}{\ln(R_\infty/r_b)}$. Notice that the value of h_w does not depend on the choice of t_0 as $h_w(t_0)$ is adjusted appropriately. The leakage is then characterized by two parameters only: the decay time τ and the far-field hydraulic head h_∞. This is as complex a model as is warranted by the available data.

[16] We calibrate the model of equation (2) using different subsequences of the data of November 2005 in order to find a range of possible values. Using intervals of 6–8 days duration starting at times between Nov. 15 and Nov. 26 yields a range of fit parameters given by the series of curves in the shaded portion of Figure 3. Even though this simple, steady-state model should only be valid for short times, it fits the observed data quite well for 3 months after the pumping.

[17] Figure 4 shows the remaining signal in hole B after the leakage modeled by equation (2) is removed. The first-order exponential trend seen in Figure 3 explains the data

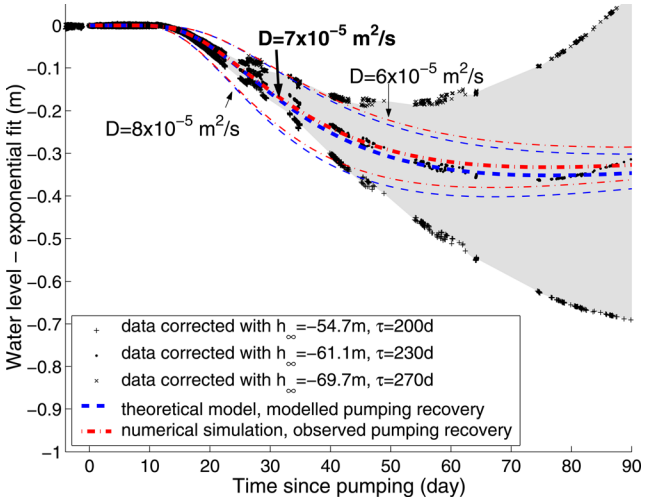

Figure 4. Pumping from hole A observed in hole B. We removed the fit of Figure 3 for the range of parameters described in section 3.2. The extreme parameters are τ = 200 days, $h_\infty = -54.7$ m and τ = 270 days, $h_\infty = -69.7$ m. In all cases, a residual anomaly begins 12 days after pumping. The auxiliary material explains the observed anomaly as the propagation of the disturbance along the fault zone with a hydraulic diffusivity $D = 7 \times 10^{-5}$ m^2/s (bold lines), using two different methods: (1) a numerical simulation with the true data from hole A, and (2) an analytical method based on the exponential fit of the recovery data in hole A of Figure 2. Modeled curves for $D = 6 \times 10^{-5}$ m^2/s (upper thin lines) and $D = 8 \times 10^{-5}$ m^2/s (lower thin lines) provide estimates of the accuracy of our value of hydraulic diffusivity. A set of intermediate parameters gives a candidate experimental curve that would be fitted by the expected curves for $D = 7 \times 10^{-5}$ m^2/s.

until 12 days after the pumping in hole A. Twelve days is longer than the duration of any of the calibration intervals. For the entire probable range of parameters, the anomaly in hole B is in the shaded region of Figure 4. In all cases, the anomaly begins suddenly 12 days after the pumping in hole A. The amplitude of the anomaly reaches at most 70 cm, about 90 days after the pumping.

3.3. Hydraulic Diffusivity From the Hydraulic Anomaly Recorded in the Observation Well

[18] We now use our fit of the water level in hole A to predict the anomaly in the corrected water level in hole B.

[19] The anomaly in hole B cannot be explained with models involving a single aquifer that both refills hole A and empties hole B. For instance, the direct application of the standard model of *Cooper et al.* [1967] gives a best fitting curve with a maximum amplitude of 4 m, five times larger than observed. Also, the observations in section 3.1 indicate that hole A is predominantly filled by an aquifer that is separate from the perforated fault zone.

[20] Instead we use a Green function solution that propagates the anomaly from hole A to hole B through a separate aquifer than the one responsible for the recovery of hole A (see auxiliary material). The model can be used to compute analytically the anomaly in hole B as long as an

analytical form is available for the input in hole A. The model has a single parameter: the hydraulic diffusivity of the damaged zone.

[21] Figure 4 shows that the modified model fits the observed anomaly with the hydraulic diffusivity $D = 7 \times 10^{-5}$ m^2/s. The input signal used for the computation is the exponential approximation of the recovery in hole A (Figure 2). This approximation has a slower recovery than the observed signal and the calculated anomaly in hole B is expected to be slightly larger than observed.

[22] The prediction is refined with numerical methods in order to use directly the time series of the water level data of hole A of Figure 2 instead of its exponential approximation. Our numerical solution was obtained by the direct implementation of equations (A1) to (A3) of the auxiliary material with the finite elements method software Comsol 3.2. With solutions using both modeled and observed recoveries in hole A, the best fit is obtained with $D = (7 \pm 1) \times 10^{-5}$ m^2/s.

4. Discussion

4.1. Identification of the Tested Aquifer

[23] We interpreted the data as the propagation of the pressure front induced by pumping within an aquifer. But which aquifer? Figure 1 suggests three main options: (1) a flow from the leak of hole A to the leak of hole B, (2) a flow between the perforations of one hole and the leak of the other hole, (3) a flow between the perforations of the two holes.

[24] The observed signal might come from the propagation of the pressure disturbance between the leaks of the two holes. However, the leakage of hole A, where water goes into the borehole, differs from the leakage in hole B, where water flows out of the borehole. Moreover, the value of diffusivity found from the cross-hole experiment is much smaller than the one derived for the leakage in hole A. These two observations suggest that the aquifer tapped by the leaks in hole A is not connected to the leak in hole B.

[25] The observed signal might also be due to a connection between the leak of one hole to the perforations of the other hole. In hole A, a cement bonding log shows that the cement in the annular interval between the casing and the borehole wall is missing at the fault zone depth but also reveals that cement plugs of good quality exist over 10 m in the annular interval at 1000 m and 1040 m. The perforations in hole A are therefore decoupled from the permeable Kueichulin formation. No such log exists for hole B. However, if the cement were very poor all along the casing on hole B, the perforations in hole B would have allowed water from the Cholan formation to enter the borehole with a rate similar to the one observed in hole A. This is not what has been observed.

[26] The most plausible hypothesis is a flow between the two perforations of the borehole located at the fault zone. Core studies [*Lockner et al.*, 2005; *Tanikawa et al.*, 2005] suggest that the fault zone has the permeability pattern described by *Caine et al.* [1996]: a fault core less permeable than the host rock, bounded by a damaged zone of enhanced permeability. Since the Chinshui shale is a relatively low permeability rock, it is probable that the easiest path between the perforations is the zone of highest permeability: the damaged zone of the Chelungpu fault. Because of the weak cement in the annular interval of hole A, the impermeable fault core is short-circuited and does not disturb the propagation of the head anomaly from the perforations of hole A (above the fault core) to the perforations of hole B (below the fault core).

4.2. Estimation of the Permeability of the Fault-Damaged Zone

[27] Most hydromechanical models studying the effect of fault zone deal with permeability. To extract this parameter from the hydraulic diffusivity, the storativity or the specific storage are needed (the storativity S is the specific storage S_s in 1/m, integrated over the thickness of the aquifer b: $S = S_s b$). For the black material forming the fault core, *Lockner et al.* [2005] found a specific storage ranging from 1.3 to 7×10^{-7} m^{-1}. However, this highly deformed material differs from the silty shale forming the matrix of the damaged zone. *Chen et al.* [2005] obtained a narrow range of specific storages of 8×10^{-7} m^{-1} to 3×10^{-6} m^{-1} on core samples of host rock far from the fault. Large scale media should be more porous and less rigid than core samples as the specific storage of poroelastic media is given by:

$$S_s = \left(\frac{\phi}{K_f} + \frac{1}{K_s}\right) \rho_f g \tag{3}$$

where ϕ is the porosity, ρ_f is the fluid density, g is the gravity acceleration, K_f and K_s are the bulk modulus of water and solid matrix respectively. In the damaged zone, the porosity and the matrix compressibility are expected to be higher than for the host rock. The specific storage might then range from 10^{-7} m^{-1} (laboratory values) to 10^{-5} m^{-1} (large scale value from equation (3)). As cores and logs suggest, the densely damaged zone has a thickness $b \simeq 1$ m. The storativity lies in the range $S = S_s\, b \simeq 10^{-7}$–$10^{-5}$.

[28] The transmissivity $T = D \times S$ is then deduced to be between 10^{-11} m^2/s and 10^{-9} m^2/s. Transmissivity T is related to permeability κ through the equation $T = \kappa\, b\, \rho_f g/\eta$ where b is the thickness of the aquifer, ρ_f is the density of the fluid and η is the dynamic viscosity of the passing fluid. For water at 50°C and $b \simeq 1$ m, the permeability is between 10^{-18} m^2 and 10^{-16} m^2. This permeability range is larger than the value 10^{-19} m^2 to 10^{-21} m^2 obtained for core samples from the fault slip zone [*Lockner et al.*, 2005] but it is not much larger from siltstone reference samples [*Chen et al.*, 2005]. *Chen et al.* [2005] found a noticeable permeability anisotropy, ranging from 10^{-19} m^2 transversely to bedding and 10^{-18} m^2 parallel to bedding.

4.3. Estimation of the Overpressure of the Fault-Damaged Zone

[29] The overpressure in the fault zone is estimated from the change in flow rate in hole B. In hole B, the rate of water level decrease changed after the perforation of the casing. Prior to perforation, the water level dropped by 24.5 cm/day. After the perforation, the water level decreased only to 22 cm/day. This corresponds to a change in flow rate $\Delta Q = 5 \times 10^{-9}$ m^3/s. Assuming an influence radius $R_\infty = 10^5\, r_b \simeq 8000$ m in equation (1) (as R_∞ is inside a logarithmic function, the result is little sensitive to the choice of this parameter), the overpressure in the

well is computed to be between 0.06 MPa (0.2% of the lithostatic pressure) and 6 MPa (20% of the lithostatic pressure).

5. Conclusion

[30] We found that the hydraulic diffusivity of the damaged zone around the Chelungpu fault is close to 10^{-4} m^2/s. This is to our knowledge the first in situ measurement of hydraulic diffusivity obtained for the damaged zone very near a major crustal fault, as similar experiments performed on other fault drilling projects give rather properties of the aquifers surrounding the fault [*Kitagawa et al.*, 1999, 2002; *Cornet et al.*, 2004].

[31] Our results suggest also that the fault damaged zone is at most moderately overpressurized (at most 20% of the lithostatic pressure), so that the fault recovery which occurred so far did not contribute to the pressure build-up. Much small overpressure is also consistent with our data.

[32] By extrapolating storativity values of core samples, the permeability is constrained to be at most 10^{-16} m^2, one hundred times the value obtained for unfractured core sample of the host rock. Observations on crystalline rock masses suggest that fracturing enhances the permeability by a factor of 100 to 1000 [*Townsend and Zoback*, 2000; *Manning and Ingebritsen*, 1999]. The permeability enhancement of the damaged zone of the fault is then in the lower part of this range. Core samples show extensive calcite crystallization in the breccia zone. A possible explanation of the small enhancement of permeability of the damaged zone is that the recovery of the fault zone is well advanced only 6 years after the Chichi earthquake.

[33] Is the observed hydraulic diffusivity small enough to maintain the pore pressure inside the fault during an earthquake? A naive interpretation suggests that fluid will begin to leak in a time equal to L^2/D, where L is the thickness on the zone of intensive shear during the earthquake, which is at most equal to the thickness of the damaged zone. For our observed values of hydraulic diffusivity and a 1 m wide damaged zone, this leakage time is a couple hours long, much longer than the duration of the earthquake. More careful formulations by *Andrews* [2002] and *Rempel and Rice* [2006] still allow pressurization to occur with the observed diffusivity D. Thermal or hydrodynamic pressurization during rupture is still a plausible mechanism.

[34] **Acknowledgments.** We thank Ji-Hao Hung for his information on the wells. We thank Chang-Wei Tsao, "Sonata" Wu, and Hsin-I Lin for their helpful activity on drill site. We are grateful to Andy Fisher for his thoughtful remarks. We thank also Joe Andrews for his constructive suggestions. M. L. Doan and E. E. Brodsky were funded in part by the National Science Foundation. Y. Kano was partially funded by the Kyoto University Active Geosphere Investigations for the 21st Century Center of Excellence (KAGI21).

References

Andrews, D. (2002), A fluid constitutive relation accounting for thermal pressurization of pore fluid, *J. Geophys. Res.*, *107*(B12), 2363, doi:10.1029/2002JB001942.

Ben-Zion, Y., and C. G. Sammis (2003), Characterisation of fault zones, *Pure Appl. Geophys.*, *160*, 677–715.

Caine, J. S., J. P. Evans, and C. B. Forster (1996), Fault zone architecture and permeability structure, *Geology*, *24*(1), 1025–1028.

Chen, N., W. Zhu, T. F. Wong, and S. Song (2005), Hydromechanical behavior of country rock samples from the Taiwan Chelungpu Drilling Project, *Eos Trans. AGU*, *86*(52), Fall Meet. Suppl., Abstract T51A–1324.

Cooper, H. H., J. D. Bredehoeft, and I. S. Papadopulos (1967), Response of a finite-diameter well to an instantaneous charge of water, *Water Resour. Res.*, *3*(1), 263–269.

Cornet, F. H., M. L. Doan, I. Moretti, and G. Borm (2004), Drilling through the active Aigion Fault: The AIG10 well observatory, *C. R. Geosci.*, *336*(4–5), 395–406.

Kitagawa, Y., N. Koizumi, K. Notsu, and G. Igarashi (1999), Water injection experiments and discharge changes at the Nojima Fault in Awaji Island, Japan, *Geophys. Res. Lett.*, *26*(20), 3173–3176.

Kitagawa, Y., K. Fujimori, and N. Koizumi (2002), Temporal change in permeability of the rock estimated from repeated water injection experiments near the Nojima fault in Awaji island, Japan, *Geophys. Res. Lett.*, *29*(10), 1483, doi:10.1029/2001GL014030.

Kitamura, K., M. Takahashi, K. Masuda, H. Ito, S. Song, and C. Wang (2005), The relationship between pore-pressure and the elastic-wave velocities of TCDP cores, *Eos Trans. AGU*, *86*(52), Fall Meet. Suppl., Abstract T51A–1326.

Lockner, D. A., C. Morrow, S. Song, S. Tembe, and T. Wong (2005), Permeability of whole core samples at Chelungpu Fault, Taiwan TCDP scientific drillhole, *Eos Trans. AGU*, *86*(52), Fall Meet. Suppl., Abstract T43D–04.

Ma, K. F., C. Wang, J. H. Hung, S. Song, H. Tanaka, E. Yeh, and Y. Tsai (2005), Dynamics of Chi-Chi earthquake rupture: Discovery from seismological modeling and Taiwan Chelungpu-Fault Drilling Project (TCDP), *Eos Trans. AGU*, *86*(52), Fall Meet. Suppl., Abstract T13A–1353.

Manning, C. E., and S. E. Ingebritsen (1999), Permeability of the continental crust: Implications of geothermal data and metamorphic systems, *Rev. Geophys.*, *37*(1), 127–150.

Nur, A., and J. Booker (1972), Aftershocks induced by pore fluid flow?, *Science*, *175*, 885–887.

Rempel, A. W., and J. R. Rice (2006), Thermal pressurization and onset of melting in fault zones, *J. Geophys. Res.*, doi:10.1029/2006JB004314, in press.

Rice, J. R. (2006), Heating and weakening of faults during earthquake slip, *J. Geophys. Res.*, *111*, B05311, doi:10.1029/2005JB004006.

Sibson, R. H., J. M. Moore, and A. H. Rankin (1975), Seismic pumping: A hydrothermal fluid transport mechanism, *J. Geol. Soc. London*, *131*(6), 653–659.

Tanikawa, W., T. Shimamoto, H. Noda, and H. Sone (2005), Hydraulic properties of Chelungpu, Shuangtung and Shuilikeng fault zones and their implications for fault motion during 1999 Chi-Chi earthquake, *Eos Trans. AGU*, *86*(52), Fall Meet. Suppl., Abstract T43D–08.

Townsend, J., and M. D. Zoback (2000), How faulting keeps the crust strong, *Geology*, *28*(5), 399–402.

E. E. Brodsky and M. L. Doan, Earth Science Department, Earth and Marine Sciences Building, University of Santa Cruz, 1156 High Street, Santa Cruz, CA 95064, USA. (ebrodsky@es.ucsc.edu; mdoan@es.ucsc.edu)

Y. Kano, Disaster Prevention Research Institute, Kyoto University, Gokasho, Uji, Kyoto 611-0011, Japan. (kano@eqh.dpri.kyoto-u.ac.jp)

K. F. Ma, National Central University, Chung-li 320-54, Taiwan. (fong@rupture.gep.ncu.edu.tw)